Supplementary Material for

Inhibition of cyclic oligomer formation via rare earth coordination and long-chain amine end capping during PA6 synthesis process

Junting Gao[a, b], Feng Gao[a, b], Ke Liu [a, b, *], Wenxing Chen[a, b], Wangyang Lu[a, b, *]

[a] State Key Laboratory of Bio-based Fiber Materials, Zhejiang Sci-Tech University, Hangzhou 310018, China

[b] Zhejiang Provincial Innovation Center of Advanced Textile Technology, Shaoxing, 312000, China

Corresponding Author:

*(K. Liu) E-mail: liuke@zstu.edu.cn.

*(W. Lu) E-mail: luwy@zstu.edu.cn; Phone: +86 0571 86843611; Fax: +86 0571 86843611.

The PA6-C obtained from the final polymerization in the factory contains 7.90wt% C1 and 3.34wt% cyclic oligomers (C_2 was 0.82wt%). Due to the different aggregation equipment, we adjusted the polymerization process to obtain slices similar to PA6-C. The ring-opening temperature (260 °C), polymerization temperature (250 °C), water (2.0wt%) and PTA (0.375wt%) addition amount are all the same as the production process of PA6-C. As shown in Figure S1 and Table S1, the C_1 was 8.42wt% when the polymerization time was 2.5 h. With further extension of polymerization time, the change in C_1 was not significant. Therefore, by further adjusting the ring opening time to 2.5 hours, W-pPA6-C with C1 and cyclic oligomers contents very similar to PA6-C were obtained, as shown in Figure S2 and Table S2. This indicated that the effect of ring-opening time on the small molecule content of PA6 was more remarkable. The content of C1 and total cyclic oligomers in W-pPA6-C was 7.92wt% and 3.36wt%, respectively.

Table S1. The contents of oligomers (C1-C9) in samples at different ring-opening and polycondensation times when the ring-opening and polycondensation temperatures were 260 °C and 250 °C, respectively.

Ring-opening time (h)	Polycondensation time (h)	Content (wt%)			Cyclic oligomer content (wt%) (C2-C9)
		C1	C2	C3-C9	
1.5	2.0	9.09	0.65	2.45	3.10
1.5	2.5	8.42	0.66	2.48	3.14
1.5	3.5	8.15	0.63	2.62	3.25
2.0	2.5	8.17	0.71	2.50	3.21
2.5	2.5	7.92	0.79	2.57	3.36
PA6-C		7.90	0.82	2.52	3.34

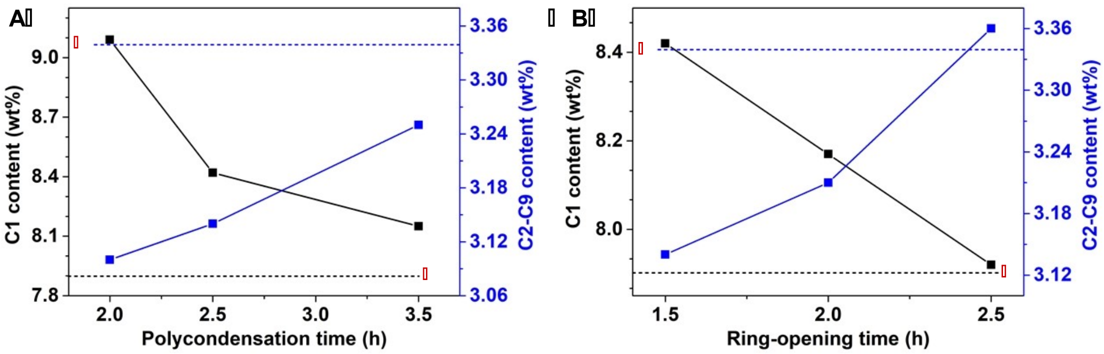

Figure S1. (A) The contents of C1 and cyclic oligomers (C2-C9) in samples at different polycondensation times when the ring-opening time was 1.5 h, (B) The contents of C1 and cyclic oligomers (C2-C9) in samples at different ring-opening times when the polycondensation time was 2.5 h. The ring-opening and polycondensation temperatures were 260 °C and 250 °C, respectively. (Line 1: the contents of cyclic oligomers in PA6-C, line 2: the C_1 in PA6-C.)

Table S2. The contents of oligomers (C1-C9) in samples at different ring-opening times when the ring-opening and polycondensation temperatures were 220 °C and 250 °C, respectively.

Ring-opening time (h)	Polycondensation time (h)	Content (wt%)			Cyclic oligomer content (wt%) (C2-C9)
		C1	C2	C3-C9	
2.5	2.5	9.90	0.30	1.99	2.31
3.0	2.5	9.29	0.31	1.98	2.29
3.5	2.5	8.26	0.34	2.07	2.41
4.0	2.5	7.62	0.35	2.09	2.46
W-pPA6-C		7.92	0.79	2.57	3.36

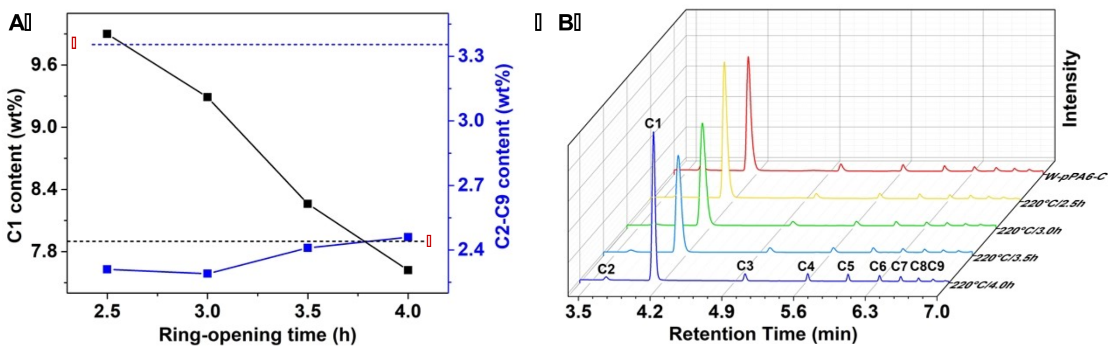

Figure S2. The contents (A) and HPLC curve (B) of C1 and cyclic oligomers (C2-C9) in samples at different ring-opening times when the polycondensation time was 2.5 h. The ring-opening and polycondensation temperatures were 220 °C and 250 °C, respectively. (Line 3: the contents of cyclic oligomers in W-pPA6-C, line 4: the C_1 in W-pPA6-C.

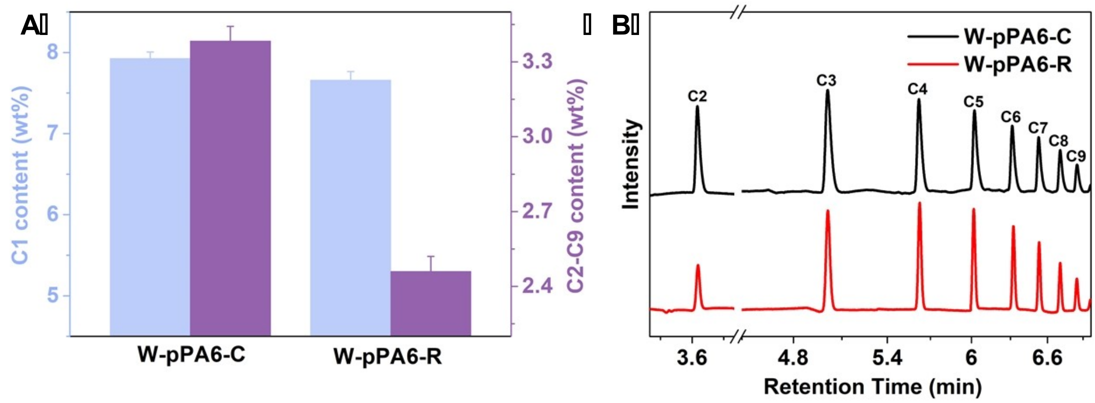

Figure S3. The contents of oligomers (C1-C9) (A) and HPLC curve of cyclic oligomers (C2-C9) (B) in PA6 samples at different ring-opening temperatures.

Table S3. The contents of oligomers (C1-C9) in samples at different ring-opening temperatures.

	Ring-opening time (h)	Polycondensation time (h)	Content (wt%)			Cyclic oligomer content (wt%) (C2-C9)
			C1	C2	C3-C9	
W-pPA6-C	2.5	2.5	7.92	0.79	2.57	3.36
W-pPA6-R	4.0	2.5	7.62	0.35	2.09	2.46

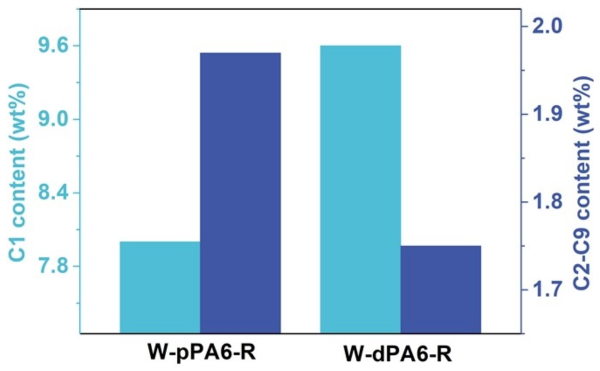

Figure S4. The contents of C1 and cyclic oligomers (C2-C9) in samples under different capping agents during the ring-opening.

Table S4. The contents of oligomers (C1-C9) in samples under different capping agents only after the end of the ring-opening reaction.

	Ring-opening time (h)	Content (wt%)			Cyclic oligomer content (wt%) (C2-C9)
		C1	C2	C3-C9	
W-dPA6-R	5.5	9.60	0.19	1.56	1.75
W-pPA6-R	4.0	8.00	0.24	1.73	1.97

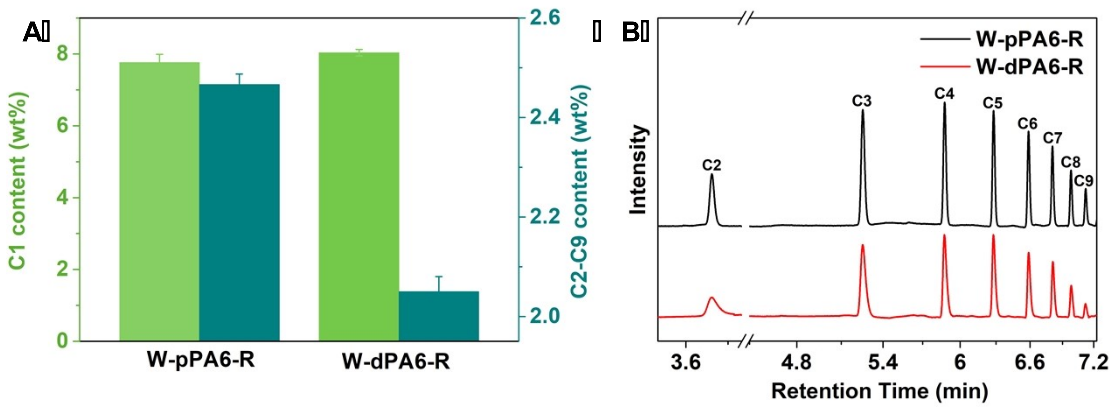

Figure S5. The contents of C1-C9 (A) and HPLC curve of C2-C9 (B) in PA6 samples under different capping agents.

Table S5. The contents of oligomers (C1-C9) in samples under different capping agents when the ring-opening and polycondensation temperatures were 220 °C and 250 °C, respectively.

	Ring-opening time (h)	Polycondensation time (h)	Content (wt%)			Cyclic oligomer content (wt%) (C2-C9)
			C1	C2	C3-C9	
W-dPA6-R	5.5	2.5	8.02	0.26	1.79	2.05
W-pPA6-R	4.0	2.5	7.62	0.35	2.09	2.46

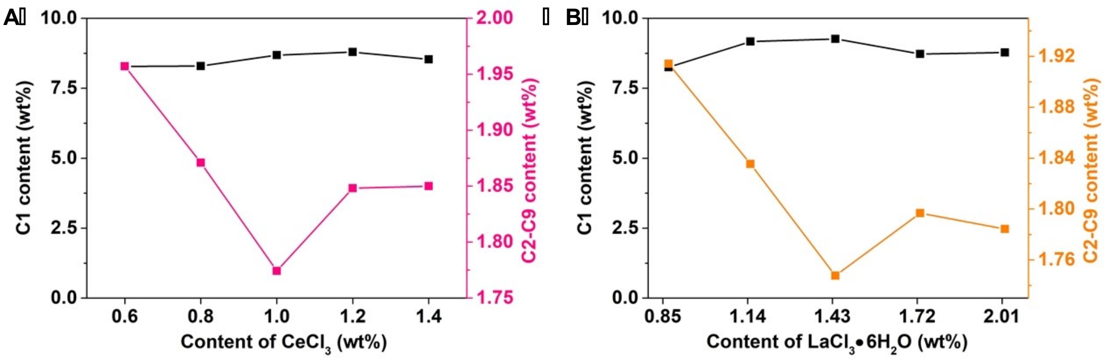

Figure S6. The contents of C1-C9 in W-Re-dPA6-R at different contents of $CeCl_3$ (A) and $LaCl_3$•$6H_2O$ (B).

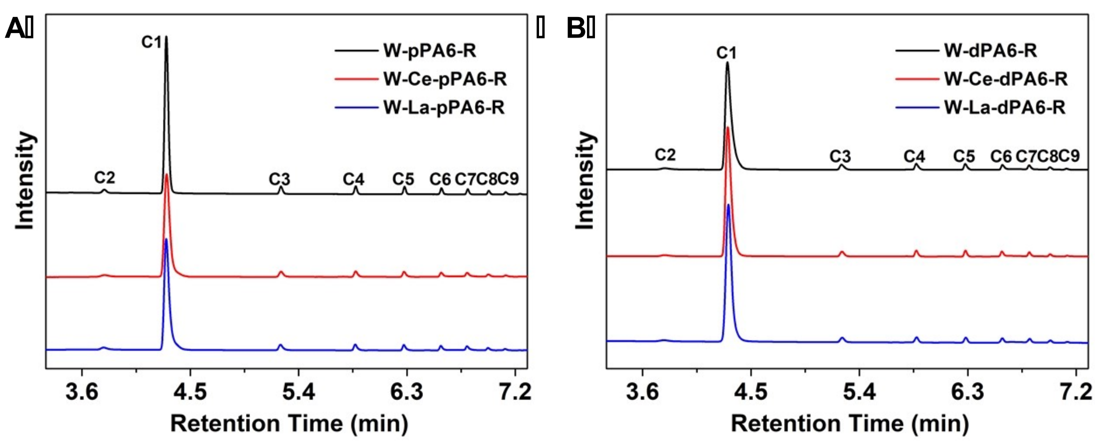

Figure S7. The HPLC curve of the species and distribution of oligomers in samples containing 1.00wt% $CeCl_3$ and 1.44wt% $LaCl_3$•$6H_2O$ under different capping agents.

Table S6. Relative viscosity and molecular weight of different PA6 samples.

Sample	Relative viscosity	M_n (g/mol)	M_w (g/mol)	*MWD*
PA6-C	2.80	24490	40600	1.751
W-pPA6-C	2.76	24410	37130	1.521
W-pPA6-R	2.70	23630	35220	1.490
W-La-pPA6-R	2.05	14710	19980	1.358
W-Ce-pPA6-R	2.07	15630	21120	1.351
W-dPA6-R	2.64	23540	38810	1.649
W-La-dPA6-R	2.01	14070	21500	1.528
W-Ce-dPA6-R	2.09	14830	22320	1.505

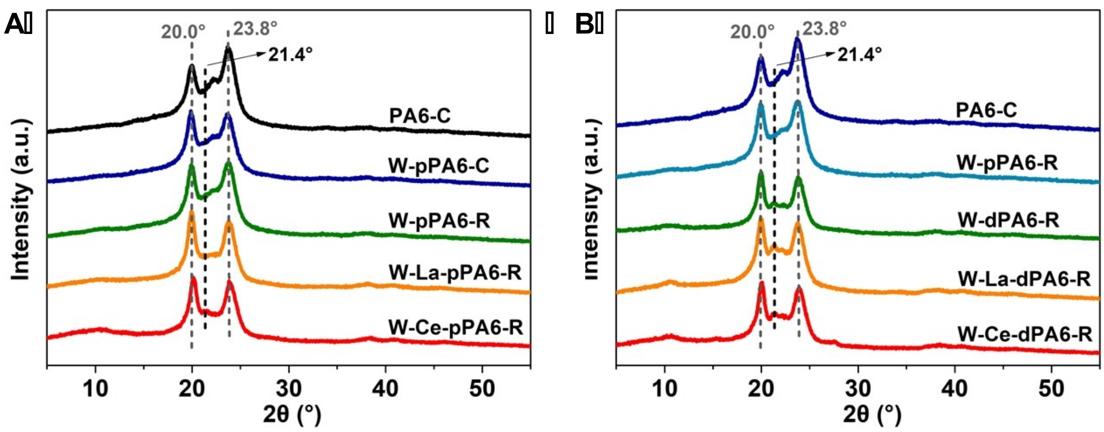

Figure S8. XRD images of different PA6 samples.

The preparation method of Ce/PA6 composite films was as follows: PA6 with a relative viscosity of 2.4 and different amounts of $CeCl_3$ were dissolved in HFIP. Then the solution was flattened on a watch glass and evaporated overnight, followed by hot pressing to prepare Ce/PA6 composite films.

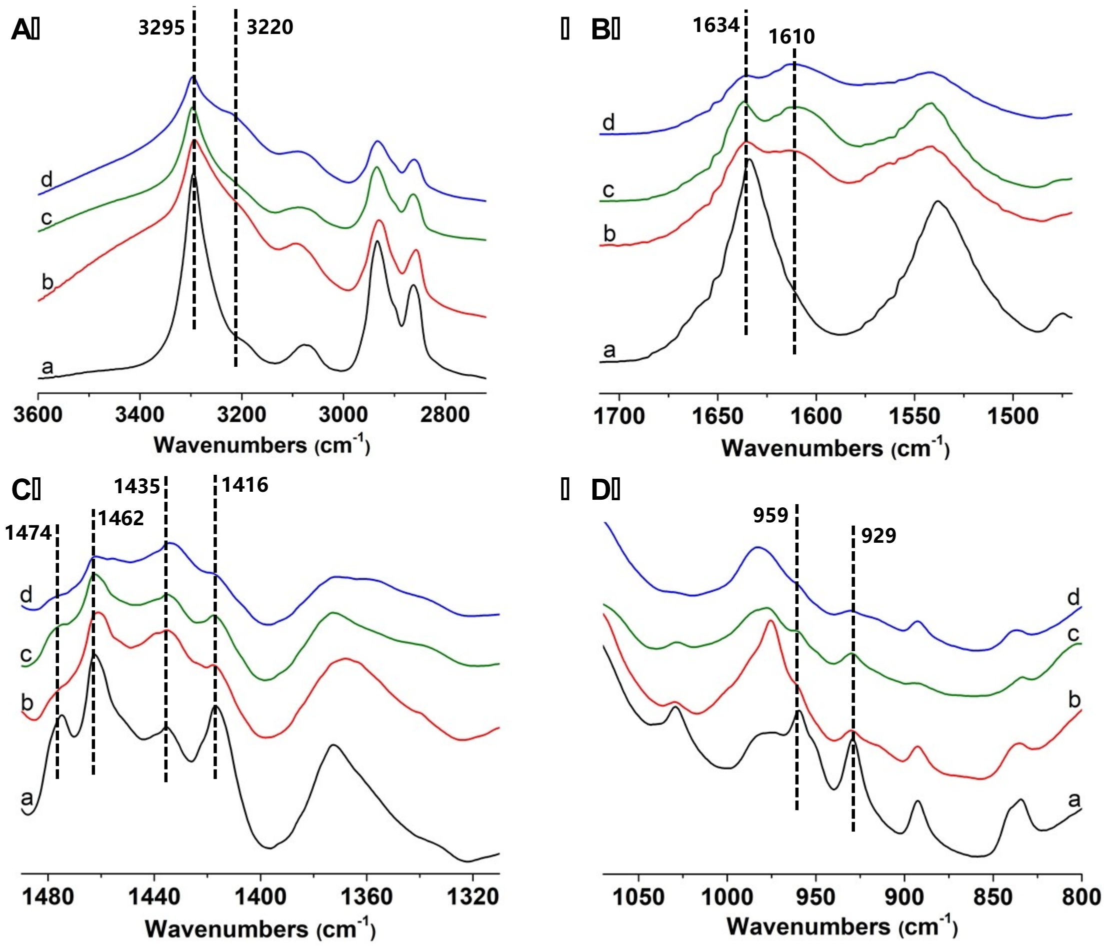

Figure S9. FTIR images of Ce/PA6 composite films. (a) pure PA6, (b) m(PA6:$CeCl_3$)=1:0.2, (c) m(PA6:$CeCl_3$)=1:0.4, (d) m(PA6:$CeCl_3$)=1:0.6.

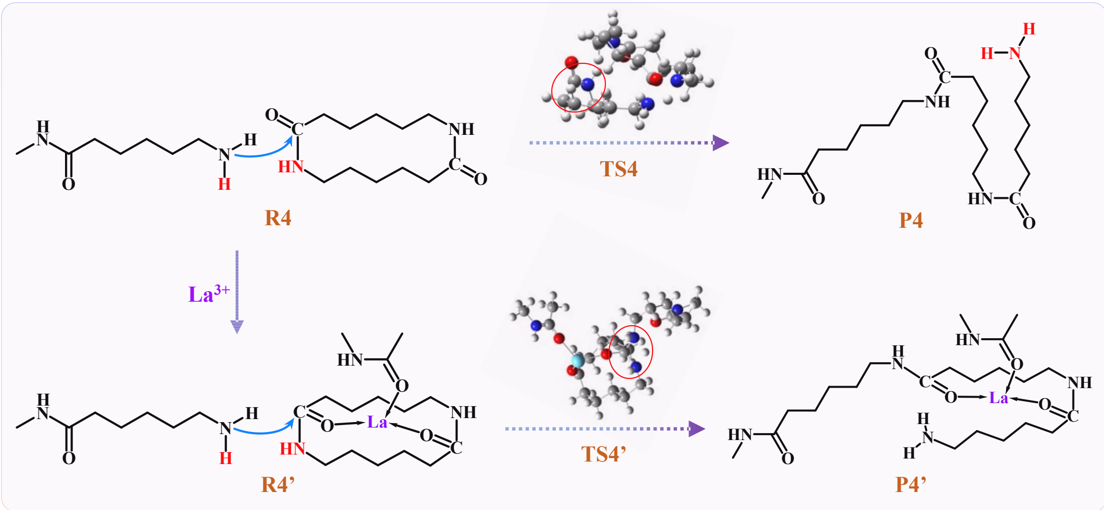

Figure S10. Proposed mechanism for the ring-opening reaction of the cyclic dimer before and after coordination with La^{3+}.

Table S7. Free energy barriers (ΔG, in kcal/mol) for the formation of C2 before and after coordination with La^{3+}.

Reactant	Transition-state	ΔG (kcal/mol)
R4	TS4	54.16
R4’	TS4’	40.83

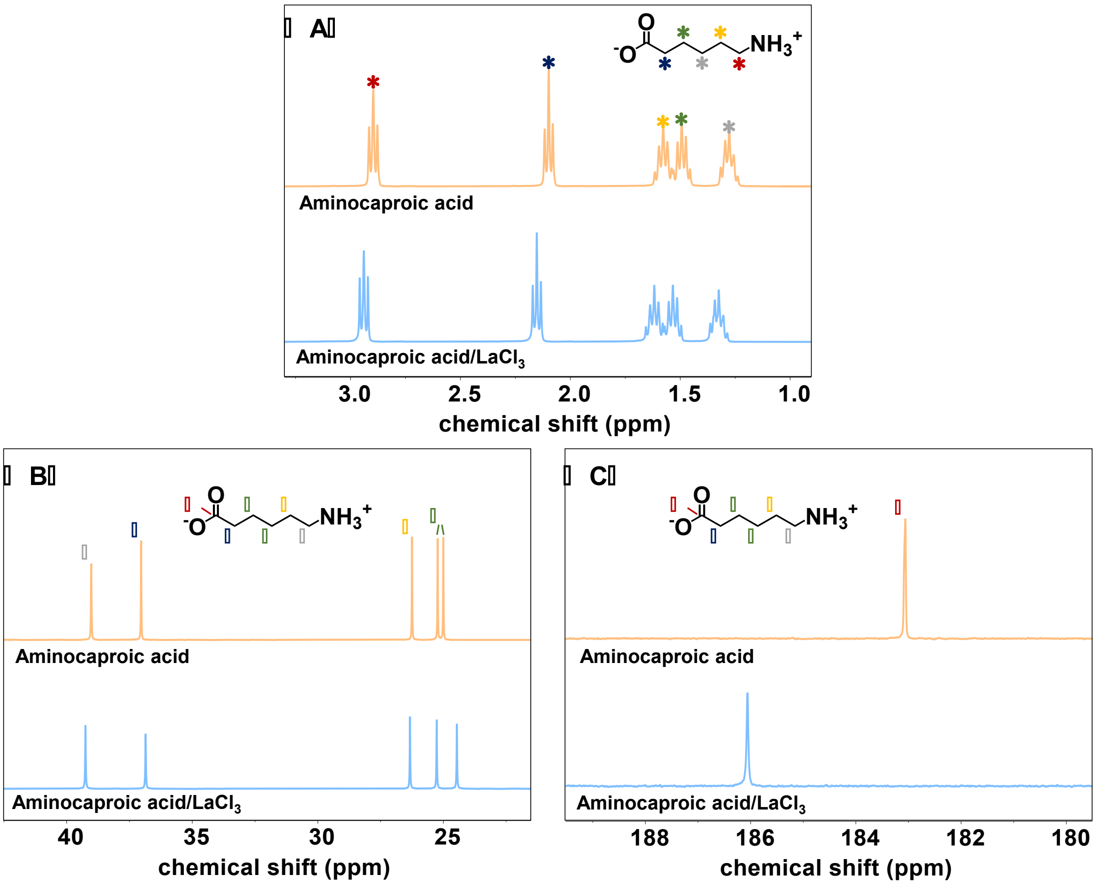

Figure S11. ^{1}H NMR (A) and ^{13}C NMR (B, C) of aminocaproic acid before and after coordination with La^{3+}.

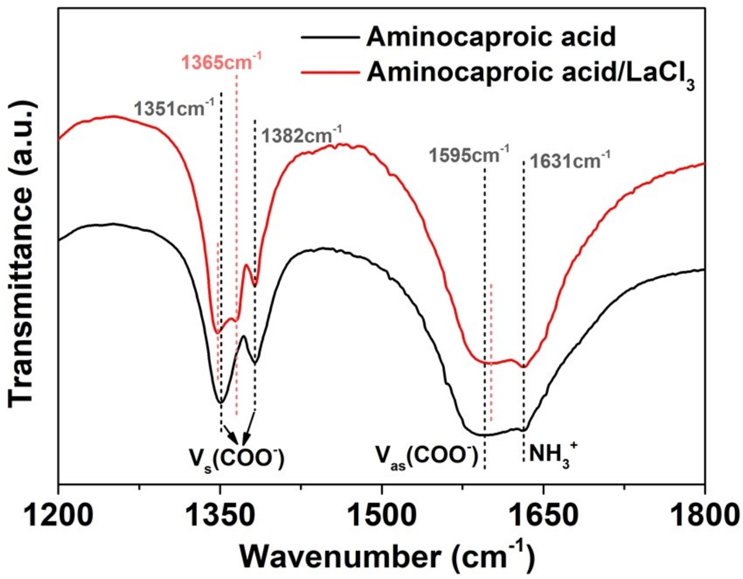

Figure S12. FTIR spectra of coordination between aminocaproic acid and La^{3+}.

Table S8. TGA data of different PA6 samples.

Sample	$T_{5\%}$ (°C)	$T_{95\%}$ (°C)	Residue (wt%)
PA6-C	375.3	470.4	0.17
W-pPA6-C	377.7	470.2	-0.77
W-pPA6-R	372.6	470.1	0.62
W-La-pPA6-R	370.2	457.5	-0.88
W-Ce-pPA6-R	370.3	457.5	-0.47
W-dPA6-R	390.7	472.8	-0.53
W-La-dPA6-R	370.2	460.1	-0.09
W-Ce-dPA6-R	357.3	460.0	0.24

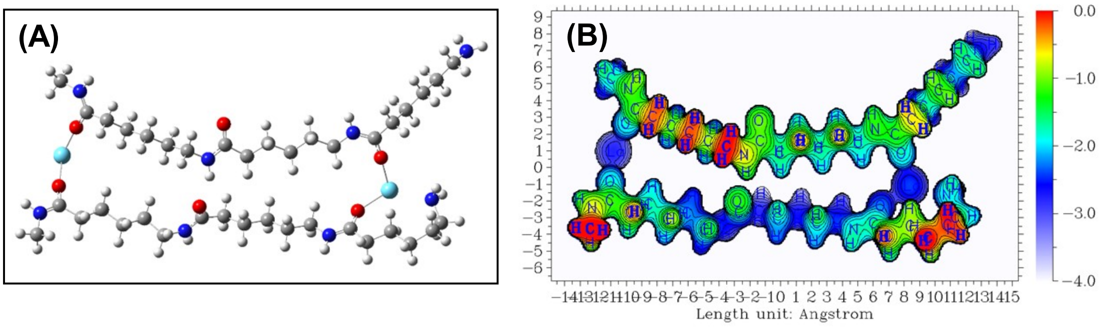

Figure S13. The chemical structure diagram of PA6 coordinated with La^{3+}.

Our study aims to reduce the content of cyclic oligomers in PA6 by adjusting the polymerization raw materials and processes, replacing the traditional hot water extraction process. The entire aggregation time has been shortened from 55 h to 10 h, resulting in a nearly 450% increase in production efficiency. Due to the fact that this study is still in the small-scale experimental stage, the energy savings are mainly estimated based on the data provided by PA6 production enterprises as support. According to the data provided in the production line records, approximately 710 kWh of electricity was consumed for every 1000 kg of PA6 produced. Therefore, we calculated the energy consumption of three quantifiable process stages (hot water extraction, drying, and remelting) based on the synthesis of 1000 kg PA6.

The traditional hot water extraction process includes hot water extraction (extraction at 110 °C for 24 h), drying (nitrogen drying at 130 °C for 24 h), and slice remelting. The hot water extraction process uses a continuous extraction tower, with a water to slice ratio of approximately 0.9:1 (extracted water can be recovered by 80% through evaporation concentration). Here, the electricity consumption of extracting water through evaporation and concentration has not been taken into account. The drying process adopts closed cycle spray drying, and the nitrogen flow is 1.2 m^3/kg. 90% of the nitrogen can be recycled, and only 10% of fresh nitrogen needs to be replenished (nitrogen density of 1.25 kg/m^3). Therefore, for every 1000 kg of PA6 produced, our method can save nearly 180 L of water (1000×0.9×0.2) and 150 kg of fresh nitrogen (1.2×1000×0.1×1.25). The specific electric energy saving estimation includes the following three parts:

(1) The hot water extraction process involves heating water from room temperature (25 °C) to extraction temperature (110 °C), which consumes approximately 88.87 kWh of electric energy.

$$Q1 = m1 \times c1 \times \triangle T$$

where m_1 is the quality of water (900 kg), c_1 is the specific heat capacity of water (4.182 kJ/kg•k), and $\triangle$T is the temperature difference (85 k).

(2) The total electricity consumption for slice drying is 12.55 kWh. Among them, heating nitrogen from room temperature (25 °C) to drying temperature (130 °C)

consumes about 4.55 kWh of electricity, and the electricity consumption of the circulation system is about 8 kWh.

$$Q2 = m2 \times c2 \times \triangle T$$

where m_2 is the quality of fresh nitrogen (150 kg), c_2 is the specific heat capacity of nitrogen (1.041 kJ/kg•k), and △T is the temperature difference (105 k).

(3) The remelting process involves heating PA6 from room temperature (25 ℃) to spinning temperature (265 ℃), which consumes approximately 126.67 kWh of electric energy.

$$Q3 = m3 \times c3 \times \triangle T$$

where m_3 is the quality of PA6 (1000 kg), c_3 is the specific heat capacity of PA6 (1.9 kJ/kg•k), and △T is the temperature difference (240 k).

According to calculations, the total electricity consumption of the three quantifiable processes in the hot water extraction step is approximately 228.09 kWh (88.87+12.55+126.67). Therefore, based on the three quantifiable processes of hot water extraction, the estimated electric energy savings are about 32.13% (228.09/710).

In addition, we estimated that approximately 14.4 kg of $LaCl_3$•$6H_2O$ was required to synthesize 1000 kg of PA6. The market price for industrial $LaCl_3$•$6H_2O$ produced by Xinsheng (Hubei) Chemical Co., Ltd. was 35 RMB/kg. Therefore, an additional expenditure of approximately 504 RMB was incurred for every 1000 kg of PA6 produced. According to economic calculations based on electricity and energy conservation, it was found that electricity was saved by approximately 182.5 RMB (average industrial electricity cost was 0.8 RMB/kWh, 228.09×0.8), and nitrogen gas for drying was saved by approximately 625 RMB (nitrogen gas was 25 RMB/6 kg, 25×25). Therefore, the total economic savings were about 807.5 RMB, which was higher than the additional cost of rare earths. In addition, the strong coordination effect of rare earths ensured their stable coordination on polymers, making them difficult to dissociate in polymers and more environmentally friendly than other heavy metals with coordination ability. In recent years, rare earths have been widely used in textile fabrics, with almost no leakage at room temperature, making their environmental pollution risk low. We further investigated the effect of rare earths on material properties and found that their mechanical properties, including tensile strength, bending strength, and impact strength, were all improved.

In this work, we employed molecular dynamics methods to investigate the effects of adding La^{3+} and Cl^{-} ions on the steric hindrance and free volume fraction of polyamide. All molecular dynamics simulations were performed using the LAMMPS software package[1] with a time step of 1 fs. The polyamide molecular chain contains 20 repeating units, and the amount of $LaCl_3$ added was 1.00wt%. The GAFF2 potential[3] was used to describe the polyamide. Intermolecular interactions were described using LJ potential and Coulombic forces, with an LJ potential cutoff radius of 1.2 nm. The PPPM method was employed to calculate long-range Coulombic forces. Initially, under the NPT ensemble, we conducted a 2 ns relaxation simulation using a Nosé-Hoover thermostat to control the temperature at 260 °C and pressure at 1 atmosphere. Subsequently, a 10 ns production simulation was performed under the same conditions, during which atomic displacements were recorded to calculate mean squared displacement (MSD), with a time window of 5 ns and processed using a moving average. Finally, the free volume fraction was calculated using the final system structure.

The MSD is defined as the average of the squared distances that the particle has traveled over a time interval (t). The MSD is given by

$$\mathrm{MSD}(t)=\frac{1}{N}\sum_{i=1}^{N}\left\langle\left|\mathbf{r}_i(t)-\mathbf{r}_i(0)\right|^2\right\rangle \quad \text{* MERGEFORMAT (1)}$$

where N is the number of particles, $\mathbf{r}_i(t)$ is the position of the i-th particle at time t, $\langle\ \rangle$ denotes the ensemble average.

The diffusion coefficient (D) is obtained from the long-time limit of the MSD,

$$D=\lim_{t\to\infty}\frac{\mathrm{MSD}(t)}{6t} \quad \text{* MERGEFORMAT (2)}$$

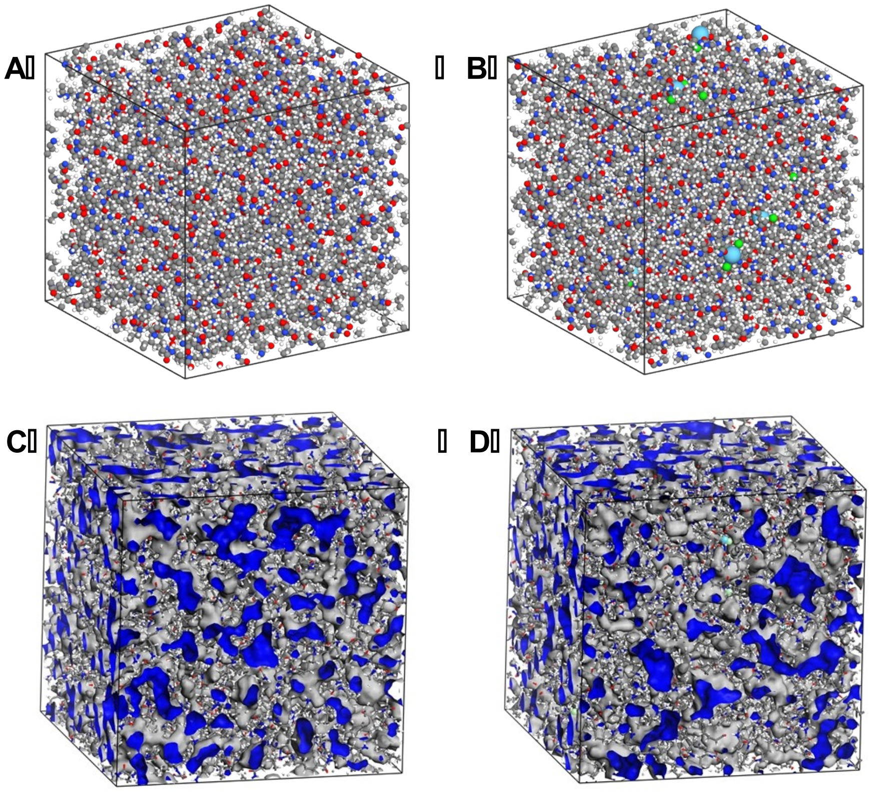

Figure S14. Schematic of simulation systems (A, B) and FFV (C, D) of PA6 segments before (A, C) and after (B, D) coordination with $LaCl_3$.

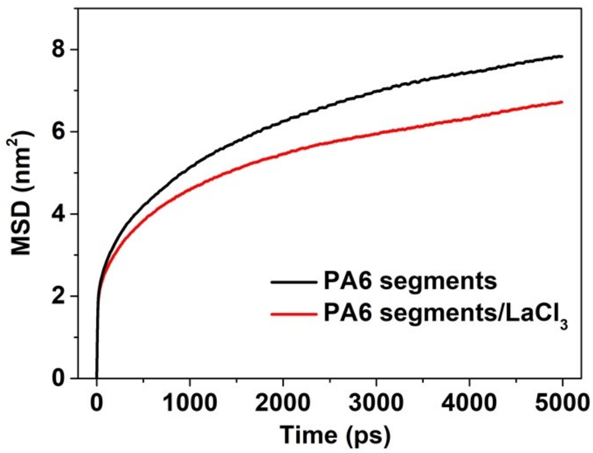

Figure S15. MSD curves of PA6 segments before and after coordination with $LaCl_3$.

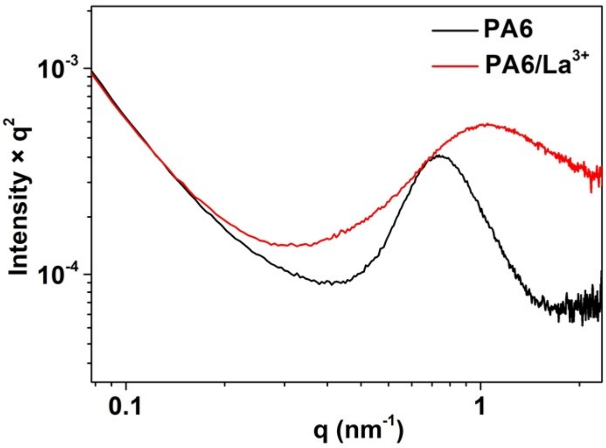

Figure S16. SAXS curve of PA6 before and after rare earth coordination.

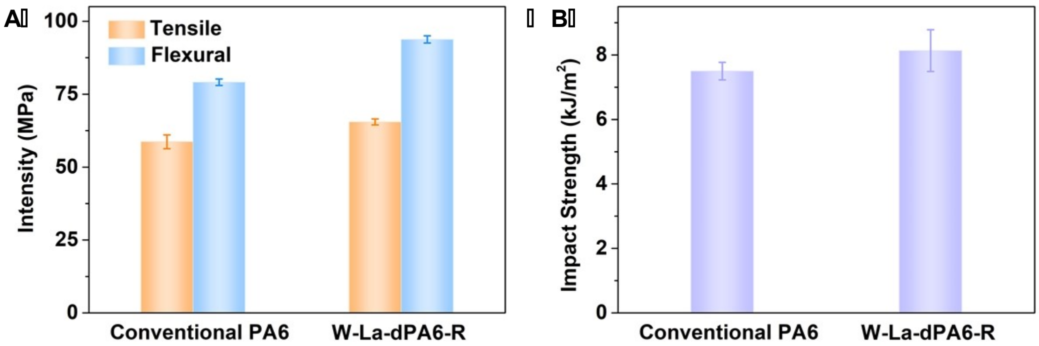

Figure S17. Mechanical properties of W-La-dPA6-R and conventional PA6.

Low molecular weight cyclic oligomers (C2~C5) have strong mobility and are prone to accumulate on the surface of fibers, leading to cracks and a decrease in fiber tensile strength. Large molecular weight cyclic oligomers (C6-C9) have difficulty moving and are prone to embedding into fibers, forming volume defects that affect long-term durability. It was worth noting that the presence of low molecular weight cyclic oligomers had a more severe impact on the mechanical properties of polymers[1]. The distribution of C3~C9 in D-Ce-dPA6-R and D-Ce-dPA6-R in this study was shown in Table S9. The total content of C3~C5 was similar to that of C6~C9, and the distribution of oligomers with different molecular weights was relatively uniform, which can minimize their adverse effects on mechanical properties.

Table S9. The content and distribution of C3~C9 in D-Ce-dPA6-R and D-La-dPA6-R.

	Content (wt%)							
	C3	C4	C5	C6	C7	C8	C9	C3~C9
D-Ce-dPA6-R	0.09	0.36	0.35	0.27	0.22	0.13	0.05	1.47
D-La-dPA6-R	0.08	0.36	0.36	0.29	0.25	0.14	0.07	1.56

Here, we injected W-La-dPA6-R before and after hot water extraction into splines to explore the correlation between the molecular weight of cyclic oligomers and the mechanical properties of polymers. The content of oligomers in W-La-dPA6-R before and after extraction was shown in Table S10, and the mechanical properties are shown in Figure S18. After hot water extraction, the content of C1~C5 in W-La-dPA6-R significantly decreased, while the content of C6~C9 remained basically unchanged. At the same time, it can be observed that the tensile strength and bending strength of the polymer significantly increased after hot water extraction, while the impact strength decreased. These results indicated that the presence of low molecular weight cyclic oligomers had an adverse effect on the tensile and flexural strength of polymers, but can improve their impact strength. Therefore, it was necessary to regulate cyclic oligomers according to application scenarios. Meanwhile, previous studies had shown that the presence of small amounts of oligomers can also serve as an "internal plasticizer" to improve melt flowability and reduce processing difficulty.

Table S10. The content and distribution of C1~C9 in W-La-dPA6-R before and after hot water extraction.

	Content (wt%)									
	C1	C2	C3	C4	C5	C6	C7	C8	C9	C1~C9
Before	9.26	0.19	0.35	0.35	0.29	0.23	0.20	0.10	0.04	11.01
After	0.72	0.06	0.15	0.18	0.20	0.21	0.20	0.10	0.04	1.86

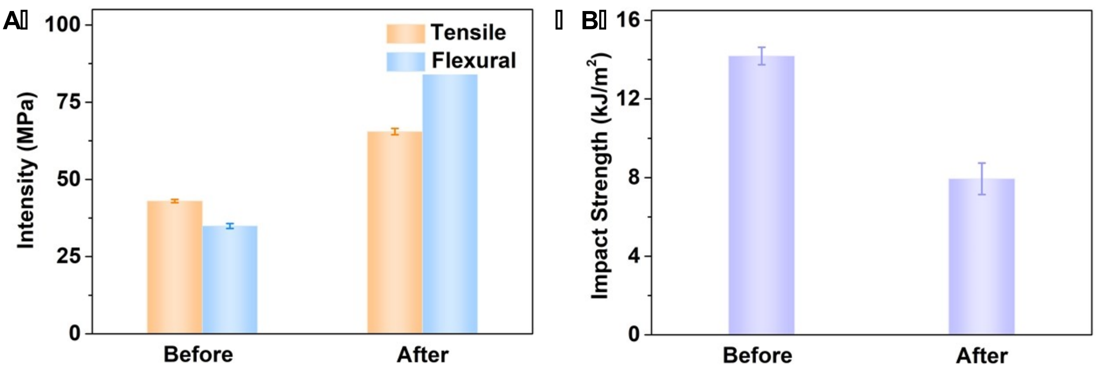

Figure S18. Mechanical properties of W-La-dPA6-R before and after hot water extraction.

Table S11. The content and distribution of different PA6 samples.

	Content (wt%)							
	C2	C3	C4	C5	C6	C7	C8	C9
W-pPA6-R	0.35	0.47	0.42	0.38	0.30	0.25	0.17	0.11
W-Ce-pPA6-R	0.27	0.43	0.38	0.34	0.23	0.23	0.13	0.06
W-La-pPA6-R	0.29	0.44	0.39	0.34	0.26	0.22	0.13	0.05
W-dPA6-R	0.26	0.41	0.38	0.35	0.25	0.22	0.12	0.05
W-Ce-dPA6-R	0.20	0.35	0.34	0.31	0.24	0.20	0.10	0.04
W-La-dPA6-R	0.19	0.35	0.35	0.29	0.23	0.20	0.10	0.04

References

[1] Wang Y, Guo Y, Zhong S, et al. Oligomer composition and content in regenerated PA6 fiber and its effect on properties[J], 2024, 141(13): e55150.